optica

Optical binding of two cooled micro-gyroscopes levitated in vacuum: supplementary material

YOSHIHIKO ARITA[1,2,*], EWAN M. WRIGHT[3,1], AND KISHAN DHOLAKIA[1,3,4,*]

[1] SUPA, School of Physics & Astronomy, University of St Andrews, North Haugh, St Andrews, KY16 9SS, United Kingdom
[2] Molecular Chirality Research Center, Chiba University, 1-33 Yayoi-cho, Inage-ku, Chiba-shi 263-0022, Japan
[3] College of Optical Sciences, The University of Arizona, Tucson, Arizona 85721-0094, USA
[4] Graduate School of Engineering, Chiba University, 1-33 Yayoi-cho, Inage-ku, Chiba-shi 263-0022, Japan
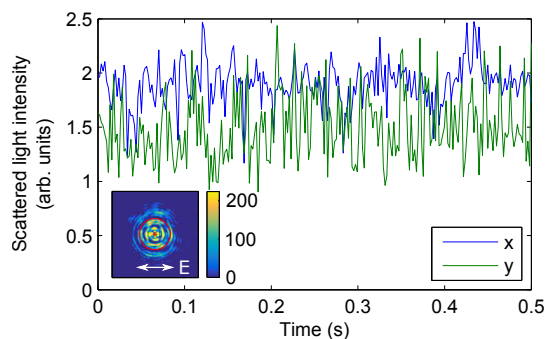[*] Corresponding authors: ya10@st-andrews.ac.uk; kd1@st-andrews.ac.uk

This document provides supplementary information to "Optical binding of two cooled micro-gyroscopes levitated in vacuum," https://doi.org/10.1364/OPTICA.5.000910.

S1. ANISOTROPIC LIGHT SCATTERING

Trapping with linearly polarized light   We investigate how the scattered light field is spatially and temporarily modulating around the particle. Figure S1 inset shows an image of the scattered light around a single vaterite particle (indicated as a red circle) trapped by a linearly polarized (LP) beam of 1070 nm. The optical axis of the birefringent particle is perpendicular to the beam axis and is aligned with the electric field E along the x axis, and hence no continuous rotation. The particle is levitated at an axial position of 15 μm above the glass coverslip inside the vacuum chamber at a vacuum pressure of 19.9 mBar. The back scattered light from the particle is collected by the same trapping objective and projected onto the fast CMOS camera, where there is no cross-polarizer in the optical path. The centre-of-mass (CoM, red cross) and the red circle with a radius of 2.2 μm are fitted to the image to determine the particle boundary. Figure S1 shows the temporal modulation of the scattered light field intensity along the x and y directions, which are comparable in magnitude (see Visualization 1 rendered at 25 fps from a measured frame rate at 500 fps). The intensity modulation represents the lateral motion of the particle (Brownian dynamics) in x and y directions.

Trapping with circularly polarized light   In contrast, the vaterite particle rotates with circularly polarized (CP) light due to spin angular momentum (SAM) transfer to the trapped particle from the trapping beam. Figures S2(a)-(g) show a series of the scattered light fields at different orientations from $0 - 2\pi$, where the field intensity modulates depending on the particle orientation. Figure S2(h) shows the temporal modulation of the scattered light along the x- and y- directions. The modulation depth is close to 100% and the intensity modulation between
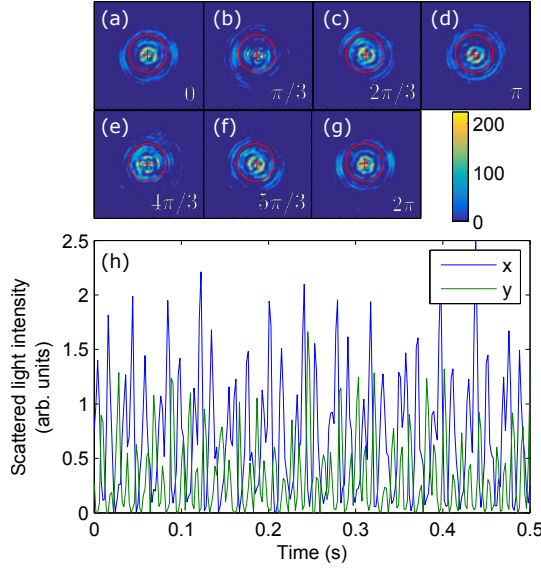

Fig. S1. Temporal modulation of the scattered light intensity along the x- (blue) and y- (green) directions around the single vaterite microparticle trapped with an LP beam in vacuum without rotation. Inset shows the scatted light around the particle with the CoM (red cross) and the particle boundary (red circle). The arrows indicate the E field along the x axis.

the x and y axes is strongly anti-correlated indicating that the rotating vaterite yields both spatially and temporally anisotropic light scattering (see also Visualization 2 rendered at 25 fps from a recorded frame rate of 500 fps). This is the basis for our assumption that the rotating particles are effectively isotropic as long as the rotation frequency far exceeds the frequencies associated with the effective optical binding.

S2. INDIVIDUAL PARTICLE DYNAMICS AND BEATING OSCILLATIONS

Trap stiffness of individual particles   In Fig. 2, we have considered the two normal-mode coordinates, namely $X_1 =$

Fig. S2. Vaterite microparticle trapped with a CP beam. (a)-(g) Scattered light fields around the particle at different particle orientation from $0 - 2\pi$. The red cross and the circle indicate the CoM and the boundary of the particle with a radius of 2.2 μm. (h) Temporal modulation of the scattered light fields along the x and y axes.

$(1/\sqrt{2})(x_1 + x_2)$ and $X_2 = (1/\sqrt{2})(x_1 - x_2)$ of the two rotating microparticles whose CoM positions are x_1 and x_2, respectively. Here we look at the CoM motion of the two individual particles in the x axis direction [see Fig. 1(a)]. Figure S3(a) shows a part of the CoM position fluctuations of the two particles with an inter-particle separation $R = 9.8$ μm. Based on the equipartition theorem, the stiffness of the traps are defined by $\kappa = k_B T / \langle \sigma^2 \rangle$, where k_B is the Boltzmann constant, $\langle \sigma^2 \rangle$ the mean square displacement of the particles. Substituting $\sigma_1 = 34.4$ nm, $\sigma_2 = 42.4$ nm and $T = 296$ K, we obtain $\kappa_1 = 3.51$ pNμm^{-1} and $\kappa_2 = 2.30$ pNμm^{-1}, respectively. These stiffness values can be used to determine the cross force constant ξ when ξ/κ is known (see Eq. 8 and Trap stiffness section).

Beating of two coupled oscillators It is intriguing to reveal how the two-rotating microparticles exhibit their translational motion when they are optically binding. Figures S3(b,c) show the normalized autocorrelation functions for the position vectors x_1 and x_2 of the two particles, where the beat note is recorded with a period of 16 ms. The corresponding beat frequency of 62 Hz is evident in the power spectra of the autocorrelation functions, where the two oscillation frequencies of $f_1 = 729.2$ Hz and $f_2 = 791.2$ Hz are both present in x_1 (green) and x_2 (red) and causing a beat note at $|f_1 - f_2| = 62$ Hz. This is a further evidence of optical binding and these two particles are no longer individual but exhibit cooperative motion via light scattering.

S3. AERODYNAMIC COUPLING DEPENDING ON DAMP-ING

In Fig. 3 we have investigated the rotational mode frequencies of the two rotating particles and have shown that the normalized DFG $2|f_{r1} - f_{r2}|/\hat{f}_r$ decreases with the decreasing damping rate of the surrounding gas molecules [see Fig. 3(d)]. This is not the case if the two particles are independent of each other and solely
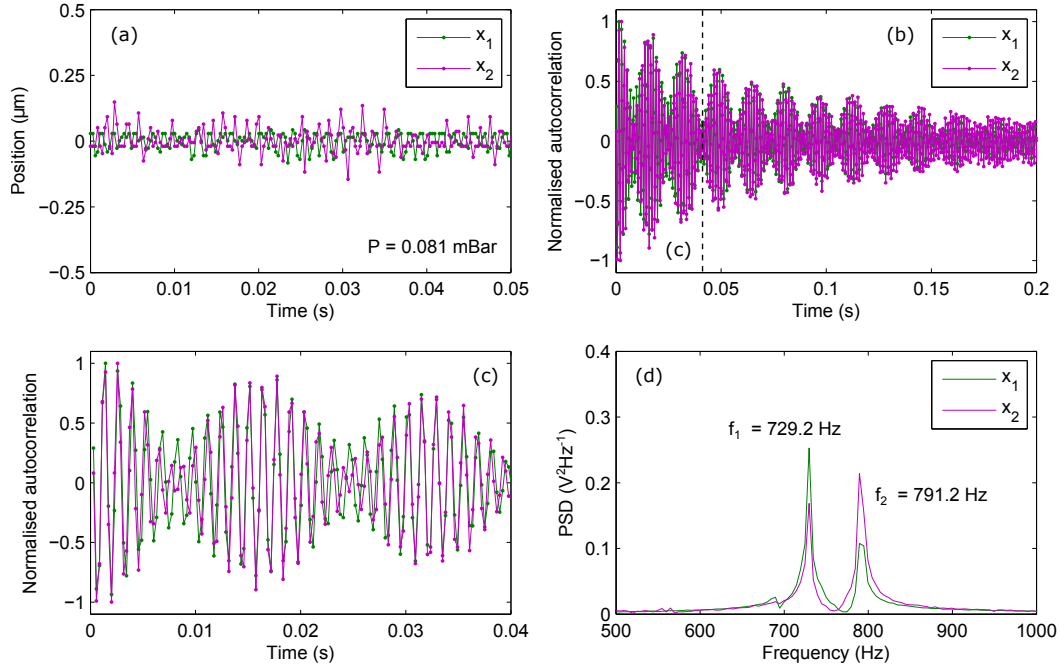
dependent on the damping rate where the normalized DFG signal should be constant over any Γ. This suggests a coupling between the two particles through residual gas molecules – aerodynamic coupling. We further investigate the relative position or the inter-particle separation R of the two particles while reducing the chamber pressure, i.e. reducing the damping rate Γ to see if the aerodynamic coupling modulates the relative position.

Line-spectra of two particles Figure S4(a) shows an image of the two particles with $R = 9.8$ μm at a residual gas pressure $P = 0.081$ mBar, which is averaged over 3493 frames acquired for 1 s [see also Fig. 3(a,b) for the position power spectrum at the same pressure]. A line-intensity profile of the two particles is measured by the cross-section across the centres of the two particles [at position $y = 0$ μm in Fig. S4(a)]. Figure S4(b) shows a series of the line-intensity profiles presented consecutively with the residual gas pressure P and with the corresponding mean rotation rate $\hat{f}_r$ of the two rotating particles. The bright diffraction rings of the particles serve as a guide for the relative position of these particles. It is evident that the two particles change the relative position depending on Γ due to the aerodynamic coupling through the residual gas molecules.
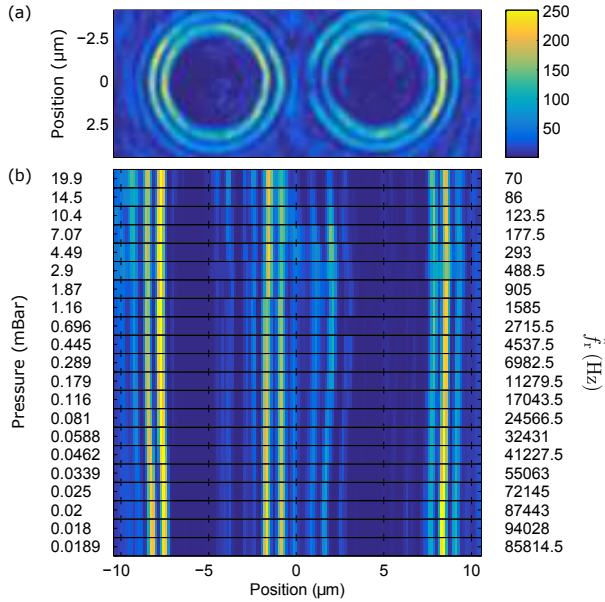
Inter-particle separation Figure S5 shows the inter-particle separation R as a function of P or the corresponding Γ. Interestingly, R increases with the decreasing P towards 1 mBar from a sub-atmospheric pressure then decreases with the decreasing P or Γ. We note that the coupling between the rotational and translational degrees of freedom of the trapped particles occurs when the rotational frequency f_{rj} is resonant with the fundamental f_j (a driven oscillator resonance) and the second harmonics $2f_j$ (a parametric resonance) of the translational frequency, where $j = 1, 2$ indicate the individual particles [S1]. As seen in Fig. 3(d) and Fig. 5(b) these resonances are responsible for various optomechanical effects, e.g. heating and cooling of the trapped particles (micro-gyroscopes). At around 1 mBar the both traps are unstable due to the resonant excitation of the trapped particles, at which condition the two particles exhibit the maximum R. Beyond this transition R decreases with the further decreasing Γ as the aerodynamic coupling or binding diminishes, where $\lambda_{mfp} \gg a \approx R$. This is in good agreement with Fig. 3(d) where ξ/κ decreases with the decreasing Γ indicating a weak dependence of ξ on the aerodynamic coupling through residual gas molecules.
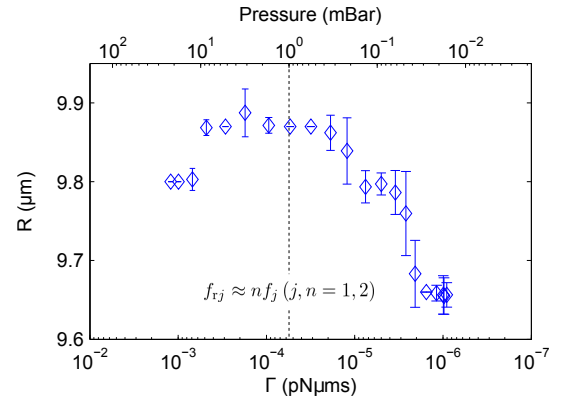
REFERENCES

[S1] Y. Arita, M. Mazilu, and K. Dholakia, "Laser-induced rotation and cooling of a trapped microgyroscope in vacuum," Nat. Commun. **4**, 2374 (2013).

Fig. S3. CoM position fluctuations x_1 (green) and x_2 (red) of two individual particles and their autocorrelation functions. (a) Position fluctuations of x_1 and x_2. (b) Normalized autocorrelation functions of x_1 and x_2. (c) An expanded view of (b) in the range of $0 \leq t \leq 0.04$ s. (d) Power spectral densities of x_1 and x_2 showing that both trapping frequencies of f_1 and f_2 are present in each particle motion.

Fig. S4. Mean relative position of the two particles. (a) An image of the two particles averaged over 3493 frames acquired in 1 s at a residual gas pressure of 0.081 mBar. (b) A series of the line intensity profiles by the cross-section across the centres of the two particles [at position $y = 0\,\mu$m] at different P and at the corresponding $\hat{f}_r$.

Fig. S5. Inter-particle separation R of the two-particle system depending on the damping rate Γ. The dashed line marks the gas pressure or the damping rate where the parametric couplings between the rotational and translational motion occur at around 1 mBar.